JOURNAL OF COMPUTATIONAL PHYSICS 37, 422–440 (1980)

Numerical Studies of Coupled Time-Dependent Diffusion Equations for the Earth's Upper Atmosphere: A Method Employing a Self-Diffusion Coefficient

G. J. BAILEY

Department of Applied Mathematics & Computing Science, University of Sheffield, Sheffield S10 2TN, England

Received April 26, 1978; revised September 18, 1979

In this paper we describe a fully time-dependent model of the Earth's mid-latitude ionospheric F2-region and protonosphere and a method for solving the coupled time-dependent continuity and momentum equations for the O^+ and H^+ ions that are associated with the model. In the method for solving the H^+ equations we employ a "self-diffusion" coefficient, a feature arising from a rearrangement of the H^+ momentum equation. An important advantage of using such a diffusion coefficient is the saving in computing time that can be achieved with little difference in the solution. To illustrate the model we present and briefly discuss a selection of results from calculations with atmospheric parameters appropriate to equinox under sunspot maximum conditions.

1. INTRODUCTION

The region of the Earth's upper atmosphere considered in this paper is the mid-latitude ionospheric F2-region and protonosphere. The F2-region, at all latitudes, is most important from the point of view of radio communication. This is because the F2-region contains the greatest concentration of free electrons, and can therefore reflect radio waves of higher frequency than can the other regions. For the purposes of this paper its lower boundary is taken to be at an altitude of 180 km. The upper boundary is not defined, but it could well be taken as the altitude where hydrogen ions (H^+) become more numerous than the oxygen ions (O^+), which predominate at the lower altitudes. This altitude, the O^+–H^+ transition altitude, is highly variable and depends, for example, upon sunspot activity, year, day, local time and location. The region where H^+ predominates is called the protonosphere.

In recent years there has been a growing interest in the coupling between the Earth's mid-latitude F2-region and the protonosphere, and the exchange of cool plasma between the two regions. Observations and calculated results indicate that such flows of ionization are often considerable. They have been discussed, for example, in connection with the question of the maintenance of the nighttime F2-region and the replenishment of ionization within the protonosphere following its

0021-9991/80/120422–19$02.00/0

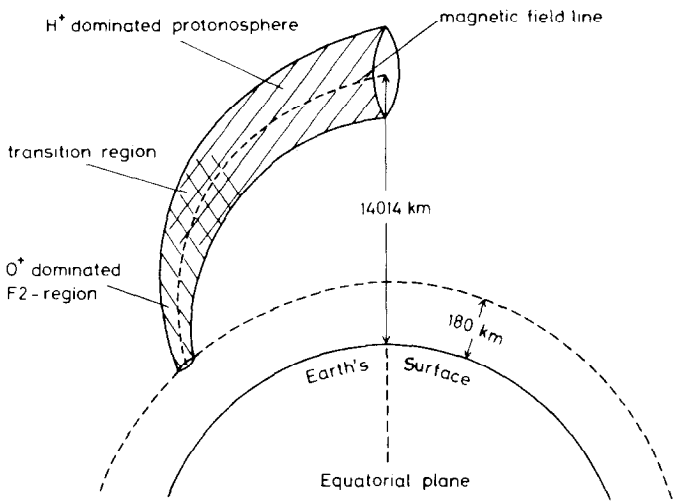

FIG. 1. Diagrammatic representation of a magnetic flux tube in the Earth's ionosphere and protonosphere (not to scale). The magnetic flux tube shown has "L value" = 3.2, i.e., the equatorial crossing point is at a distance 3.2 × Earth's radius from the Earth's centre. The cross-sectional area A of the magnetic flux tube is proportional to B^{-1}, where B is the Earth's magnetic induction field (here taken to be a dipole field).

removal during magnetic storms. A brief review of these topics and related topics is given by Evans [1].

To study the coupling between the F2-region and the protonosphere we need to know the distribution of the various ions within these two regions. This is achieved, theoretically, by solving coupled continuity and momentum equations for each ion within a magnetic flux tube. For many problems it is sufficient to consider a weakly ionized plasma consisting of the two ions O^+ and H^+ since O^+ is dominant within the F2-region and H^+ within the protonosphere (see Fig. 1). For the purposes of this paper we assume a centred dipole geomagnetic field with geographic and magnetic axes coincident and we concentrate on the magnetic flux tube associated with the $L = 3.2$ magnetic field line, where L = equatorial radial distance/radius of the Earth. The $L = 3.2$ magnetic flux tube is of particular interest since the incoherent scatter radar station at Millstone Hill, Massachusetts, USA, is associated with this value of L and the Millstone Hill station provides large quantities of observed data on a routine basis. For definiteness we normalize the magnetic flux tube to 1 cm^2 cross-sectional area at 1000 km; at the equator the cross-sectional area is 36 cm^2.

It is the purpose of this paper to present (i) a fully time-dependent model that is suitable for studying the daily behavior of the Earth's F2-region and protonosphere at mid-latitudes, and (ii) a method for solving the associated coupled O^+ and H^+ continuity and momentum equations. To illustrate the model we present and discuss a selection of results from calculations using atmospheric parameters appropriate to equinox under sunspot maximum conditions.

2. Mathematical Formulation of the F2-Region and Protonosphere

In this section we present the equations of momentum and continuity for the electrons and ions as they apply to the F2-region–protonosphere environment; that is, a partially ionized plasma moving in a neutral atmosphere under the forces of gravity, pressure gradients, and electric and magnetic fields. At mid-latitudes and for magnetically quiet conditions the flow of plasma normal to the magnetic field lines is small (see [2] and references cited therein). To a very good approximation it is therefore sufficient to consider a model with the flow of plasma parallel to a magnetic field line [3]. We assume that the magnetic flux tube, associated with the magnetic field line, corotates with the Earth.

For subsonic flows adequate approximations to the electron and ith ion momentum equations are

$$\frac{1}{N_e}\frac{\partial p_e}{\partial s} = -eE'', \tag{1}$$

and

$$\frac{1}{N_i m_i}\frac{\partial p_i}{\partial s} + g'' - \frac{eE''}{m_i} = -\sum_j \nu_{ij}(v_i'' - v_j'') + \sum_j \alpha_{ij}\frac{N_j k}{N_e m_i}\frac{\partial T_i}{\partial s}, \tag{2}$$

respectively, where

N_e = electron concentration,
N_i = ith ion concentration,
N_j = jth ion concentration ($j \neq i$),
p_e = electron pressure,
p_i = ith ion pressure,
e = electron charge,
E'' = magnetic field-aligned electric field,
m_i = ith ion mass,
g'' = magnetic field-eligned component of acceleration due to gravity,
s = distance along magnetic field line from lower boundary,
ν_{ij} = collision frequency for momentum transfer between the ith ion and the jth ion ($j \neq i$) or the jth neutral gas,
v_i'' = magnetic field-aligned component of velocity for the ith ion,
v_j'' = magnetic field-aligned component of velocity for the jth ion ($j \neq i$) or the jth neutral gas,
α_{ij} = thermal diffusion coefficient between the ith and jth ions ($i \neq j$),
T_i = temperature of the ions,
k = Boltzmann's constant.

The continuity equation for the ith ion is

$$\frac{\partial N_i}{\partial t} + \frac{1}{A}\frac{\partial A\phi_i}{\partial s} = P_i - L_i, \tag{3}$$

where

A = cross-sectional area of magnetic flux tube,
$\phi_i = N_i v_i'' = i$th ion field-aligned flux,
P_i = production rate of the ith ion,
L_i = loss rate of the ith ion,
t = time.

The area A is proportional to B^{-1}, where B is the Earth's magnetic induction field.

For the electrons

$$N_e = \sum_j N_j, \tag{4}$$

where the summation is over all ion species, since the plasma, to a good approximation, is electrically neutral.

For the model presented in this paper we assume that the ions are O^+ and H^+ and we denote by $i = 1$ the O^+ ion and $i = 2$ the H^+ ion. Thus the ith ion momentum equation ($i = 1$ and 2), obtained by eliminating eE'' from Eqs. (1) and (2) and using

$$p_i = N_i k T_i, \tag{5}$$

$$p_e = N_e k T_e, \tag{6}$$

becomes

$$0 = -g \sin I - \frac{kT_i}{m_i}\frac{1}{N_i}\frac{\partial N_i}{\partial s} - \frac{kT_e}{m_i}\frac{1}{N_e}\frac{\partial N_e}{\partial s} - \frac{k}{m_i}\frac{\partial (T_e + T_i)}{\partial s}$$
$$- \alpha_{ij}\frac{N_j k}{N_e m_i}\frac{\partial T_i}{\partial s} - \nu_{ij}(v_i'' - v_j'') - \nu_{in}(v_i'' - u\cos I), \tag{7}$$

where

g = acceleration due to gravity,
I = magnetic dip angle,
T_e = electron temperature,
u = meridional component of the neutral air wind velocity,
ν_{in} = sum of collision frequencies for momentum transfer between the ith ion and the neutral gases.

3. Previous Methods and Introduction to the New Method

There are available only a few fully time-dependent models that are suitable for studying the day-to-day behaviour of the Earth's mid-latitude F2-region and

protonosphere [2, 4–8]. All these models employ one, or a combination, of the two methods outlined below to solve the continuity and momentum equations for each ion species.

The usual method for solving time-dependent ion continuity and momentum equations is to solve the momentum equation for the field-aligned ion flux and substitute into the continuity equation to give the diffusion equation

$$\frac{\partial N_i}{\partial t} = D_{i0} \frac{\partial^2 N_i}{\partial s^2} + D_{i1} \frac{\partial N_i}{\partial s} + D_{i2} N_i + D_{i3}. \tag{8}$$

This equation is non-linear in the sense that D_{i0}, D_{i1} and D_{i2} are functions of N_i. Also, we have that the diffusion coefficient D_{i0} is very large at high altitudes and this leads to computational difficulties (see [8]). A numerical solution of Eq. (8) is usually obtained by an implicit finite-difference method (Crank–Nicolson method [9] or Laasonen method [10]). In order to overcome the instabilities in the solution which originate due to the very large diffusion coefficient we have to use very small increments in t and s, Δt and Δs, respectively. Also, the computing time is very large since the solution of the O^+ and H^+ equations is required over several days and the $L = 3.2$ magnetic flux tube is very long (approximately 22,000 km). Massa [6] used this method with $\Delta t = 1$ min and 2100 values of Δs, where the value of Δs increased exponentially with altitude, for his solution of the O^+ and H^+ equations within the $L = 3$ magnetic flux tube and with the O^+ concentration at 300 km taken from observation. He found that a 24-hr period required about 1200 sec computing time on a CDC 7600 computer.

An alternative method used by Moffett and Murphy [5] (see also Mayr *et al.* [4]) is to integrate the continuity equation for the field-aligned ion flux and substitute into the momentum equation to give an integro-differential equation for N_i. This equation is written in the form

$$\frac{\partial}{\partial s} \log N_i = \left(\frac{kT_i}{m_i} + \frac{kT_e}{m_i} \frac{N_i}{N_e} \right) \left[\frac{\nu_{ij}}{A N_i} \int_s^{s_{eq}} A \left(P_i - L_i - \frac{\partial N_i}{\partial t} \right) ds + \text{other terms} \right], \tag{9}$$

where s_{eq} is the equatorial values of s. At high altitudes ν_{ij} becomes very small. It will be seen later that the smallness of ν_{ij} leads naturally to the physically correct behaviour of N_i at high altitudes. On the other hand the lower boundary condition can only be satisfied approximately and a searching procedure is required for determining the correct equatorial value of N_i. Various studies by Bailey, Moffett and Murphy have used this searching method for the H^+ equations. For the O^+ equations these authors have used the Laasonen [10] fully implicit finite-difference method at altitudes below a selected altitude (around 1500 km for their sunspot minimum conditions, around 3500 km for their sunspot maximum conditions) with zero field-aligned flux being assumed above the selected altitude. Bailey, Moffett and Murphy found that sufficient accuracy could be obtained with $\Delta t = 15$ min and with about 200 values of Δs (very large values of Δs at high altitudes) for their sunspot minimum

calculations. In Murphy *et al.* [2] it is claimed that a 24-hr period of integration requires a modest 7 min computing time on an ICL 1907 computer, a much slower computer than the CDC 7600 used by Massa [6]. The main drawbacks of the searching method are (i) the difficulty in obtaining an accurate value for the H^+ concentration at low altitudes and (ii) the difficulty in obtaining a solution of the H^+ equations from "poor" initial conditions. Both these drawbacks usually involve considerable wastage of computer time.

For the method presented in this paper the O^+ and H^+ time-dependent continuity and momentum equations are written as diffusion equations of the form Eq. (8). However, for H^+ a preliminary rearrangement of its momentum equation is carried out in such a way that the diffusion coefficient does not become too large. This permits larger values of Δt and Δs to be used in the integration process than would otherwise be possible and, as a result, the computing time is reduced considerably. Both the O^+ and H^+ diffusion equations are solved by the Laasonen [10] fully implicit finite-difference method.

A comparison of the results using the method presented in this paper with the searching method [2] has been carried out with identical data and parameters. Using $\Delta t = 900$ sec and 953 values for Δs (see Section 4.5) we have compared the results from the first 3 days' calculations. At all altitudes and times the results for H^+ are within 6 % and for O^+ within 2 %. Exact agreement cannot be expected because the linearization procedures adopted for the H^+ equations are different for the two methods. The computing time required on the Sheffield University 1906S computer for a 24-hr period of calculations is 203 sec for the method presented in this paper and 526 sec for the searching method [2].

A further and important advantage of the method presented in this paper over the searching method is that it can be extended more easily to magnetic flux tubes that extend over two hemispheres, an essential modification for investigating interhemisphere coupling. Bailey *et al.* [11] have demonstrated a technique for extending the searching method to two hemispheres. Their technique involves three searching procedures and is very time consuming.

4. Solution of the O^+ and H^+ Continuity and Momentum Equations

4.1. O^+ *and* H^+ *Diffusion Equations*

For O^+ the O^+ field-aligned flux ϕ_1 $(=N_1 v_1'')$ is found from the O^+ momentum equation (Eq. (7) with $i = 1$) and substituted into the O^+ continuity equation (Eq. (3) with $i = 1$) to give the O^+ diffusion equation

$$\frac{\partial N_1}{\partial t} = D_{10} \frac{\partial^2 N_1}{\partial s^2} + D_{11} \frac{\partial N_1}{\partial s} + D_{12} N_1 + D_{13}, \tag{10}$$

where

$$D_{10} = R_1, \tag{11}$$

$$D_{11} = R_1 \frac{1}{A}\frac{\partial A}{\partial s} + \frac{\partial R_1}{\partial s} + S_1, \tag{12}$$

$$D_{12} = S_1 \frac{1}{A}\frac{\partial A}{\partial s} + \frac{\partial S_1}{\partial s} - \beta_1, \tag{13}$$

$$D_{13} = P_1, \tag{14}$$

and

$$R_1 = \frac{k}{m_1}\left(T_i + T_e\frac{N_1}{N_e}\right)\Big/(\nu_{12} + \nu_{1n}), \tag{15}$$

$$\begin{aligned} S_1 = \Bigg(& g\sin I + \frac{k}{m_1}\frac{T_e}{N_e}\frac{\partial N_2}{\partial s} + \frac{k}{m_1}\frac{\partial(T_e + T_i)}{\partial s} \\ & + \alpha_{12}\frac{k}{m_1}\frac{N_2}{N_e}\frac{\partial T_i}{\partial s} - \nu_{12}v_2'' - \nu_{1n}u\cos I\Bigg)\Big/(\nu_{12} + \nu_{1n}). \end{aligned} \tag{16}$$

The term β_1 in Eq. (13) is the loss rate coefficient of the O^+ ions (see Section 5).

If this approach were adopted for H^+ then the diffusion coeficient D_{20} would be proportional to $1/(\nu_{21} + \nu_{2n})$. At high altitudes ν_{2n} is negligible and ν_{21} is very small ($\nu_{21}\,\alpha\, N_1$). Thus D_{20} becomes very large at high altitudes and small values of Δt and Δs are needed for a stable solution of the H^+ equations. We make, therefore, the following modification which prevents D_{20} from becoming too large and permits larger values of Δt and Δs to be used. The modification consists of writing the term $\nu_{21}(v_2'' - v_1'')$, in the H^+ momemtum equation, in the form

$$\begin{aligned} \nu_{21}(v_2'' - v_1'') &= \nu_{21}\left(\frac{\phi_2}{N_2} - \frac{\phi_1}{N_1}\right) \\ &= \frac{\nu_{21}}{N_1}\left(\frac{N_1}{N_2}\phi_2 + \phi_2 - \phi_1 - \phi_2\right) \\ &= \frac{\nu_{21}}{N_1}\left(\frac{N_e}{N_2}\phi_2 - \phi_1 - \phi_2\right). \end{aligned} \tag{17}$$

In the numerical solution of the H^+ diffusion equation, to be described in Section 4.2, we evaluate the additional terms of Eq. (17), namely, $+\phi_2$ and $-\phi_2$, at different times. The term $+\phi_2$ is evaluated at time $t + \Delta t$ whilst the term $-\phi_2$ is evaluated at time t. Obviously, the accuracy of this approximation depends on the rate of change of ϕ_2 with respect to time and on the time step, Δt, employed. The value of ϕ_2 may change dramatically over short periods of time at around sunrise and sunset and during periods of disturbed magnetic activity. The mathematical complexity of the plasma continuity and momentum equations precludes any detailed

analysis of the accuracy of the approximation made in Eq. (17). However, we justify the approximation on geophysical grounds by referring to observational results and to the physics of the Earth's upper atmosphere. To commence with, we note that the modification is only needed at high altitudes. Thus, we use the modification only at high altitudes. At altitudes above about 1000 km there is considerable uncertainity in the values of the atmospheric parameters that have to be used in any mathematical model. From the geophysical viewpoint, therefore, we accept errors in numerical solution procedures at high altitudes which may not be permitted at low altitudes, provided that the result of the model calculations are in reasonable agreement with observation and theory. Our numerical solution procedure, which includes the modification at the higher altitudes, does give results that are in reasonable agreement with observatin and theory. Of course, the inaccuracies arising from using the modification can be reduced by decreasing Δt. A small value of Δt has to be used, irrespective of the mathematical model, when a detailed study of changes in plasma composition and motion is being performed for periods of rapidly changing atmospheric condition. The validity of the modification has been demonstrated by comparing with the searching method [2]; see Section 3. Numerical experiment has shown that a reasonable lower altitude for the introduction of the modification is the O^+–H^+ transition altitude. Thus below the O^+–H^+ transition altitude the H^+ diffusion equation is similar to Eq. (10) with the coefficients similar to Eqs. (11)–(16). Above the O^+–H^+ transition altitude Eqs. (15) and (16) become

$$R_2 = \frac{k}{m_2}\left(T_i + T_e\frac{N_2}{N_e}\right)\Big/\left(\nu_{21}\frac{N_e}{N_1} + \nu_{2n}\right), \tag{18}$$

$$S_2 = \left(g\sin I + \frac{k}{m_2}\frac{T_e}{N_2}\frac{\partial N_1}{\partial s} + \frac{k}{m_2}\frac{\partial(T_e+T_i)}{\partial s} - \alpha_{12}\frac{k}{m_2}\frac{N_1}{N_e}\frac{\partial T_i}{\partial s} - \frac{\nu_{21}}{N_1}(\phi_1+\phi_2) - \nu_{2n}u\cos I\right)\Big/\left(\nu_{21}\frac{N_e}{N_1} + \nu_{2n}\right). \tag{19}$$

At high altitudes N_2 is dominant and ν_{2n} is negligible. Thus, at high altitudes, the diffusion coefficient R_2 is essentially independent of the background gases. It is, however, dependent upon the H^+ concentration. We have chosen to call such a diffusion coefficient the *self-diffusion* coefficient.

4.2. *Numerical Method*

The equations to be solved are the two non-linear coupled partial differential equations

$$\frac{\partial N_i}{\partial t} = D_{i0}\frac{\partial^2 N_i}{\partial s^2} + D_{i1}\frac{\partial N_i}{\partial s} + D_{i2}N_i + D_{i3}, \tag{20}$$

where $i = 1$ denotes the O^+ ion and $i = 2$ the H^+ ion. These equations are non-linear and coupled in a complicated way since the coefficients D_{ij} $(i = 1, 2; j = 0, 1, 2, 3)$

are functions of various given parameters and the variables N_i ($i = 1, 2$) and their derivatives.

The non-linearity of these equations is overcome by a simple linearization process and by solving the O^+ equation before the H^+ equation. This order is essential if large values of Δt are to be used and arises because H^+ plays only a small rôle in determining the O^+ distribution whereas O^+ plays a dominant rôle in determining the H^+ distribution. An outline of the computational scheme for advancing the solution from time t to $t + \Delta t$ is as follows:

(i) calculate the coefficients D_{10}, D_{11}, D_{12}, D_{13} by using N_1, N_2, v_1'' and v_2'' from time t and the remaining atmospheric parameters from time $t + \Delta t$,

(ii) solve for N_1 by the Laasonen [10] fully implicit finite-difference method,

(iii) calculate v_1'' from the O^+ momentum equation,

(iv) calculate the coefficients D_{20}, D_{21}, D_{22}, D_{23} by using N_1 and v_1'' from time $t + \Delta t$, N_2 and v_2'' from time t; and the remaining atmospheric parameters from time $t + \Delta t$,

(v) solve for N_2 by the Laasonen [10] fully implicit finite-difference method,

(vi) calculate v_2'' from the H^+ momentum equation.

We note that in this scheme we use values calculated at time $t + \Delta t$ wherever possible.

We have justified the validity of the linearization procedure by carrying out a set of calculations, with identical data, that included an iteration procedure at each time step. For a Δt of 15 min, the value used in the present study, we found that iterating had a negligible effect on the results.

4.3. *Boundary Conditions*

The upper boundary is taken to be at the equator, where we assume zero interhemispheric O^+ and H^+ fluxes (equinoctal conditions), i.e., $\phi_1 = \phi_2 = 0$. At the equator we have, therefore, from Eq. (7)

$$0 = -R_i \frac{\partial N_i}{\partial s} - S_i N_i \qquad (i = 1 \text{ and } 2), \tag{21}$$

where the R_i and S_i are as defined in Section 4.1. Upon integrating, Eq. (21) becomes

$$N_i(s_{eq}) = N_i(s_{eq} - \Delta s) \exp\left(-\int_{s_{eq}-\Delta s}^{s_{eq}} \frac{S_i}{R_i} ds\right). \tag{22}$$

At the lower boundary, $z = 180$ km, the chemical terms P_i and L_i ($i = 1$ and 2) dominate and so we assume that

$$N_i = P_i/\beta_i \tag{23}$$

($i = 1$ and 2).

4.4. *Initial Conditions*

The solution procedure is started at 06.00 LT on Day 0 with O^+ and H^+ in chemical equilibrium (i.e., $P_i = L_i$, $i = 1, 2$) at low altitudes and diffusive equilibrium (i.e., $\phi_i = 0$, $i = 1, 2$) otherwise. The O^+ and H^+ field-aligned fluxes, ϕ_1 and ϕ_2, respectively, are taken to be zero at all altitudes. The initial altitude distribution of the O^+ and H^+ field-aligned fluxes and O^+ concentration need only be arbitrary since the effect on the results of these initial distributions decreases with time; by the end of Day 0 the effect is negligible. The initial altitude distribution of the H^+ concentration, on the other hand, determines the initial H^+ content of the magnetic flux tube and the H^+ content of the $L = 3.2$ magnetic flux tube changes slowly with time (further details are given in Section 6). The O^+ content of the $L = 3.2$ magnetic flux tube is negligible when compared with the H^+ content. For the results presented in this paper we use an initial altitude distribution for the H^+ concentration that gives a low H^+ content, characteristic of the protonosphere just after a magnetic storm [12].

5.4. *Integration Increments Δt and Δs*

Various numerical experiments have been carried out to determine suitable values for Δt and Δs taking into account accuracy and computer time and storage requirements. At altitudes where the concentrations of O^+ and H^+ vary rapidly with altitude small values of Δs are needed. At the higher altitudes O^+ varies approximately as Eq. (22) and H^+ varies slowly with altitude. As a result larger values of Δs can be used at the higher altitudes. For the results presented in this paper we have used $\Delta t = 900$ sec, and a distribution for Δs that is approximately 6 km below 3000 km and which varies linearly with altitude to approximately 60 km at the equator.

5. Atmospheric Parameters

To calculate the coefficients D_{i0}, D_{i1}, D_{i2} and D_{i3} ($i = 1$ and 2) we require values for the concentrations and temperature of the neutral gases, the ion and electron temperatures, the ion production and loss rates, the collision frequencies for momentum transfer, the neutral air wind velocity, and the thermal diffusion coefficients.

In the region of the earth's atmosphere above 120 km, the neutral gases that play important rôles in determining the production, loss and diffusion rates of the O^+ and H^+ ions are O, O_2, N_2 and H (atomic oxygen, molecular oxygen, molecular nitrogen and atomic hydrogen, respectively). The altitude variations and common temperature of these neutral gases have been calculated from formulae given by Walker [13] and, except for H, the daily variations follow Jacchia [14] with shape parameters given by Jacchia [15]. For H, the concentration at 500 km is assumed to vary sinusiodally with local time and is adjusted to the experimentally obtained values of Vidal-Madjar

et al. [16]. The daily variations at 300 km of the concentrations of O, O_2, N_2 and H, and of their common temperature, T_n, are shown in Fig. 2.

For altitudes below 1000 km the electron temperature, T_e, is based on data collected at Millstone Hill, Massachusetts, and supplied by J. V. Evans and J. E. Salah (private communication). Shown in Fig. 3 are contours of electron temperature at altitudes below 1000 km. For altitudes higher than 1000 km there is insufficient spatial coverage by experiment for a reliable T_e model to be constructed. We follow, therefore, Marubashi and Grebowsky [17] and assume that T_e varies exponentially along the magnetic field line as follows:

$$T_e = T_e^{\max} - (T_e^{\max} - T_e^{\min}) \exp(-(s - s_{1000})/A), \tag{24}$$

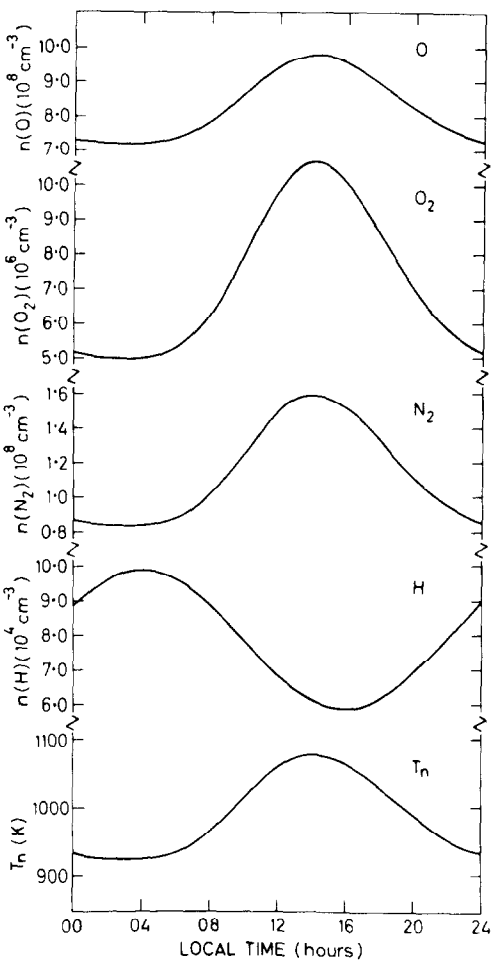

FIG. 2. The variation with local time of the concentrations of O, O_2, N_2 and H, and of T_n, at an altitude of 300 km.

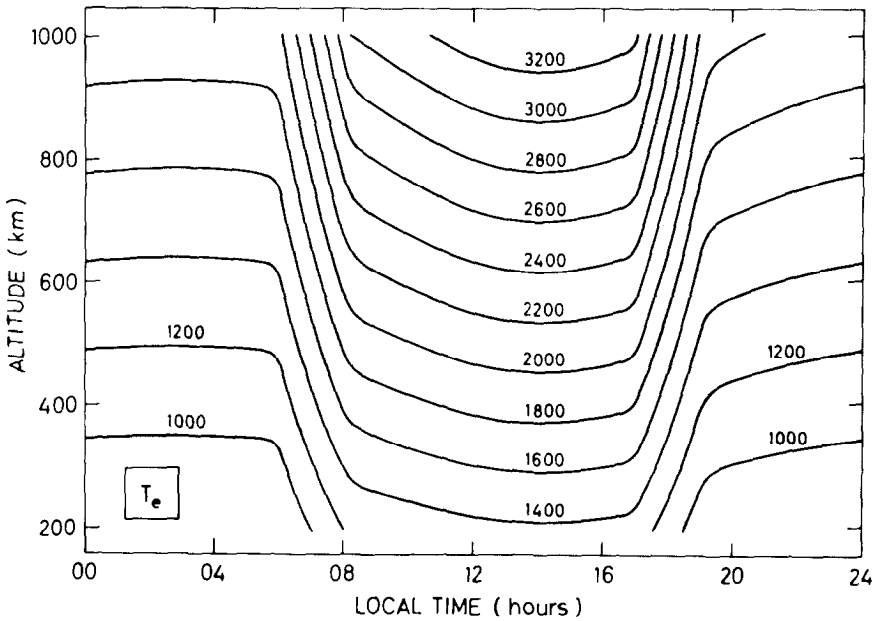

FIG. 3. Contours of electron temperature, T_e, at altitudes below 1000 km.

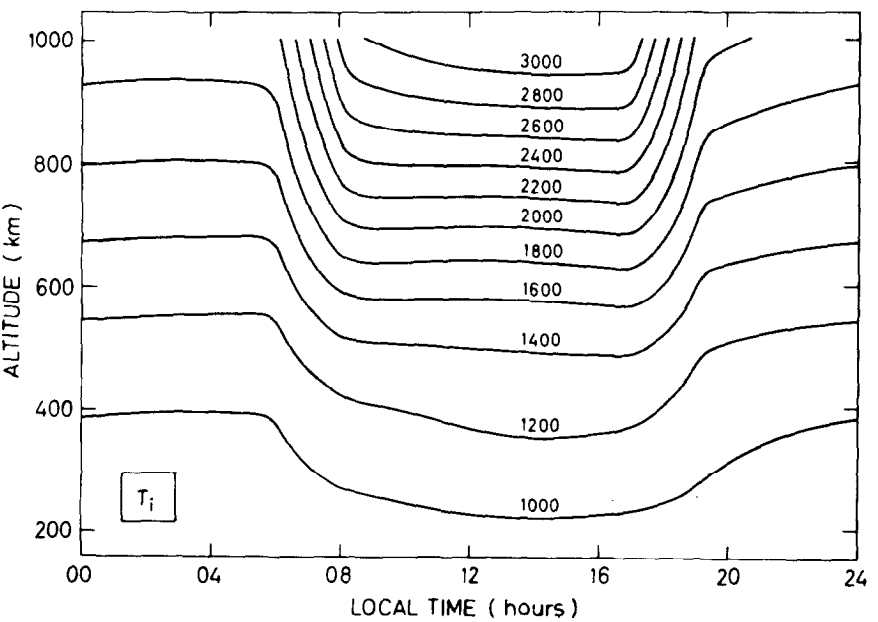

FIG. 4. Contours of ion temperature, T_i, at altitudes below 1000 km.

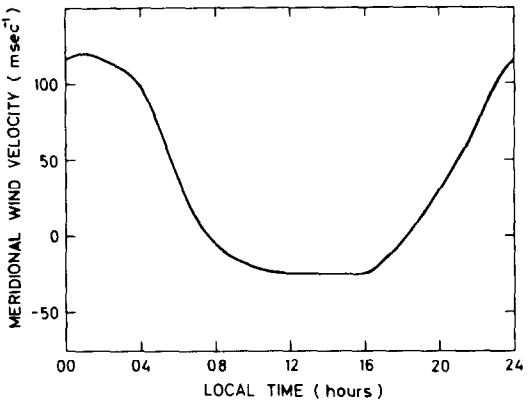

FIG. 5. The variation with local time of the meridional component of the neutral air wind velocity (constant with altitude).

where T_e^{max} varies sinusoidally with local time with a diurnal maximum of 12,000 K at 15.00 LT and a minimum of 8000 K at 03.00 LT. Such magnitudes are in reasonable agreement with the equatorial variations measured by Serbu and Maier [18]. T_e^{min} and A are dtermined from the requirement that T_e and $\partial T_e/\partial s$ be continuous at 1000 km ($s = s_{1000}$).

The ion temperature, T_i, is obtained at all altitudes by balancing the ion thermal energy input from the electron–ion collisions to that lost through collisions with the neutral particles. At high altitudes T_i equals T_e; at low altitudes T_i approaches T_n. Shown in Fig. 4 are contours of ion temperature at altitudes below 1000 km.

Oxygen ions are produced by photoionization of O by solar radiation of wavelengths below 911 Å. For the photoionization rate coefficient at the top of the atmosphere we have used $3.4 \times 10^{-7}\,\text{sec}^{-1}$. Rates for the loss of O^+ and production and loss of H^+ are given by Raitt *et al.* [19] and Roble [20]. Values for the collision frequencies for momentum transfer are given by Raitt *et al.* [19]. The thermal diffusion coefficients are evaluated from expressions given by Schunk and Walker [21].

The meridional component of the horizontal neutral air wind, although playing an important rôle in F2-region dynamics, is poorly known. For our calculations we have used a meridional wind velocity based on the calculations of Roble *et al.* [22]. It is taken to be uniform with altitude and its daily variation is shown in Fig. 5.

6. RESULTS

The daily pattern of refilling of the protonosphere after it has been depleted, for example, by a magnetic storm, is shown in Fig. 6. For the sunspot maximum conditions considered here there is a continual increase in the H^+ content of the magnetic flux tube during the first 10 days of post-storm recovery. Full recovery of

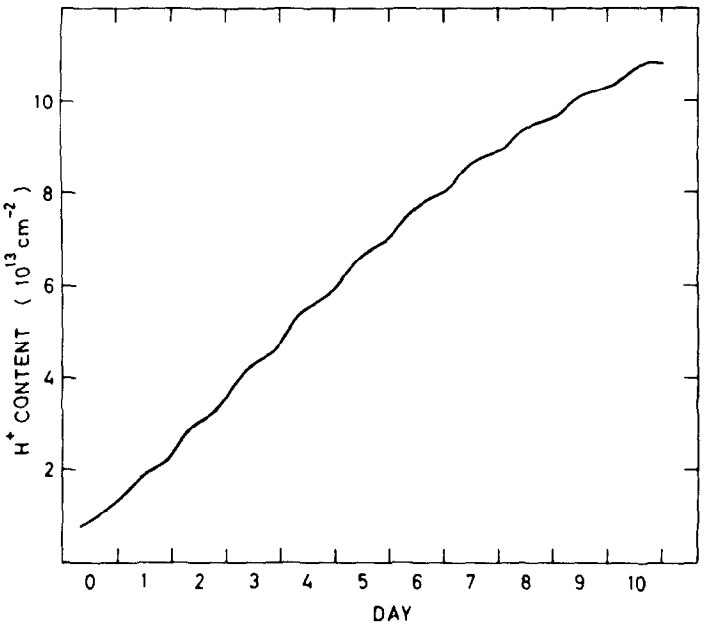

FIG. 6. Calculated daily behaviour of H^+ content within the $L = 3.2$ magnetic flux tube for successive days, showing the recovery of the H^+ content from a depleted state.

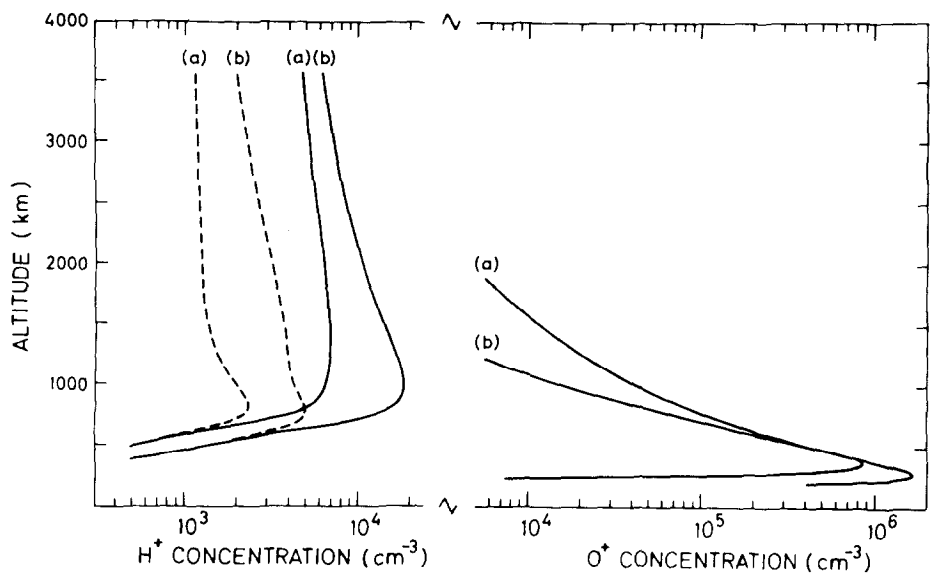

FIG. 7. Calculated altitude profiles of O^+ and H^+ concentration at 12.00 and 24.00 LT on Days 2 and 10: (a) 12.00 LT, (b) 24.00 LT; – – –, Day 2; ——, Day 10. There is little difference between the O^+ concentration profiles for Day 2 and Day 10.

the protonosphere has not yet occurred. (For full recovery a 24-hr periodic solution is required.) However, during the recovery period, the net daily gain in H^+ content decreases as time progresses. For example, during Day 1 the net gain is 1.03×10^{13} ions whereas on Day 10 the net gain is 0.56×10^{13} ions.

There are uncertainties in the data used for the present calculations, especially in the plasma temperature which influences the recovery time [2]. Nevertheless, it is most unlikely that the calculated time for full recovery of the protonosphere will become less than the time elapsing between magnetic storms, since at sunsport maximum magnetic storms occur frequently [23, 24]. Consequently, the present calculations suggest that the mid-latitude protonosphere will never recover from the depletion effects of a magnetic storm before the onset of another magnetic storm.

During the recovery period of the protonosphere the altitude variation of the H^+ concentration changes significantly (see Fig. 7) and it is strongly dependent upon the existing magnetic flux tube content. This is unlike the O^+ concentration. In the topside ionosphere and protonosphere O^+ is almost in diffusive equilibrium at all times and its concentration is controlled mainly by its peak value NmF2 lying within

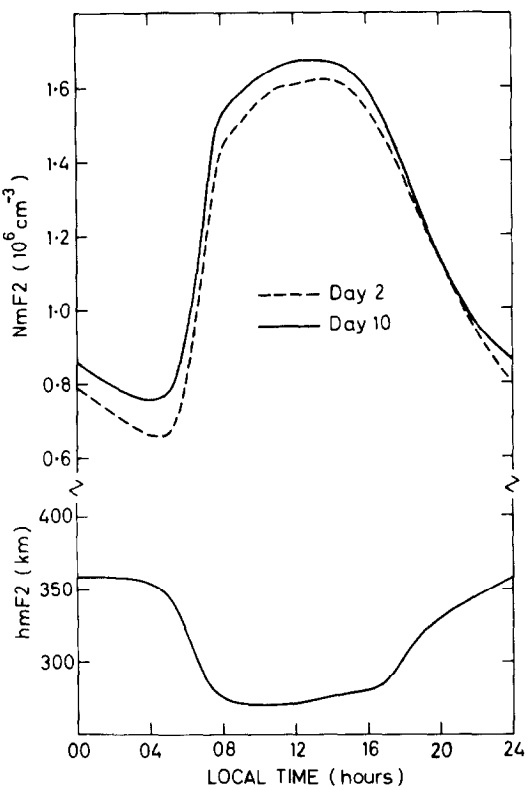

FIG. 8. Calculated daily behaviour of NmF2 and hmF2 for Days 2 and 10. There is no change in the daily behaviour of hmF2 between Day 2 and Day 10.

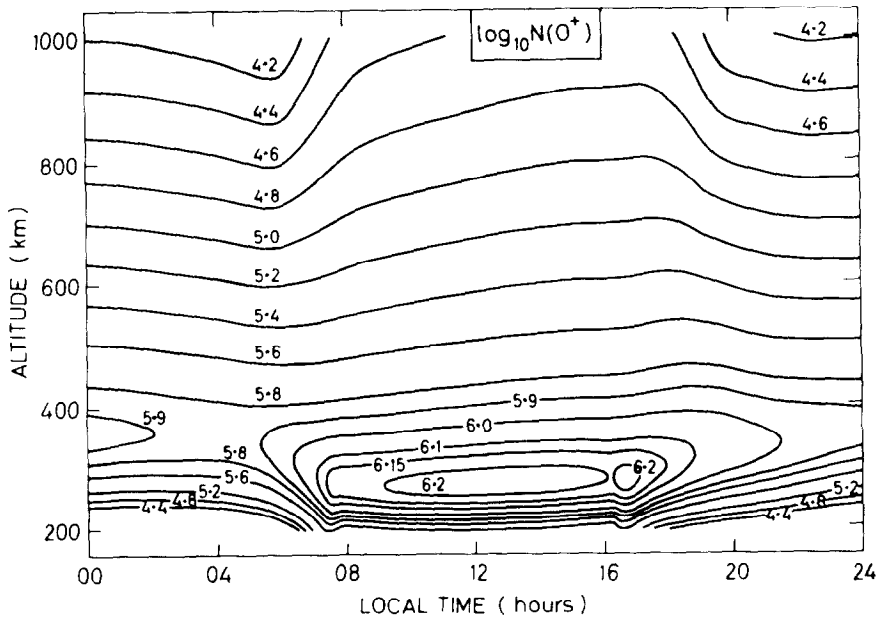

FIG. 9. Contours of $\log(N(O^+))$, where $N(O^+)$ are the calculated O^+ concentrations for Day 10.

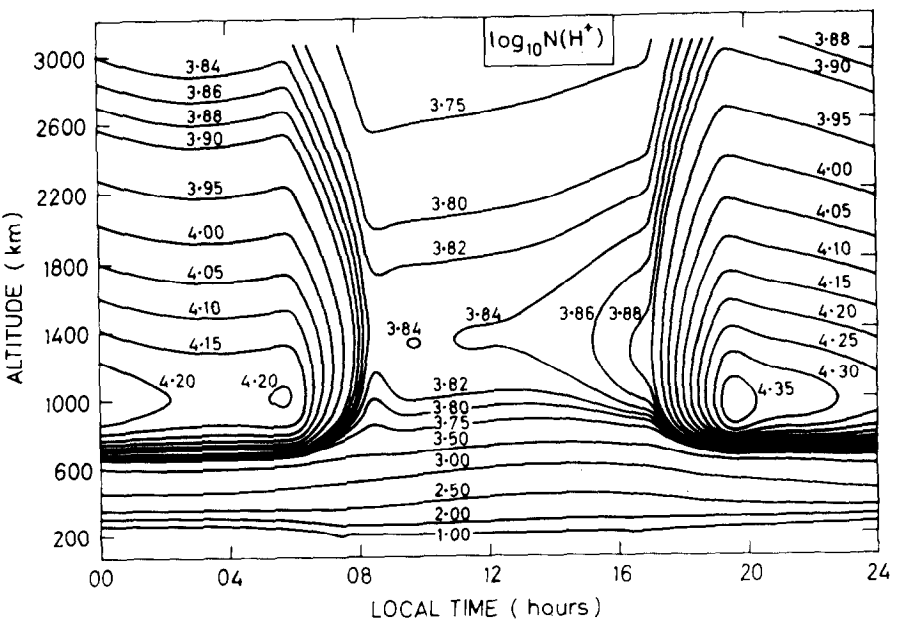

FIG. 10. Contours of $\log(N(H^+))$, where $N(H^+)$ are the calculated H^+ concentrations for Day 10.

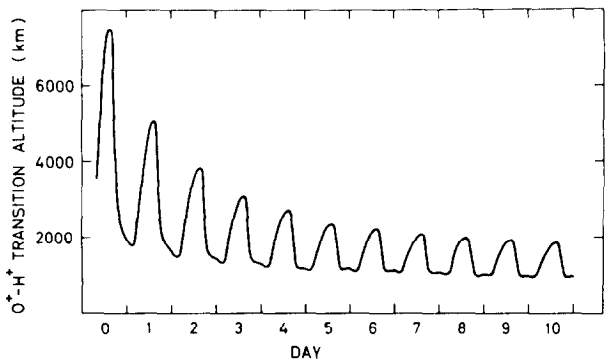

FIG. 11. Calculated daily behaviour of the O^+–H^+ transition altitude for successive days.

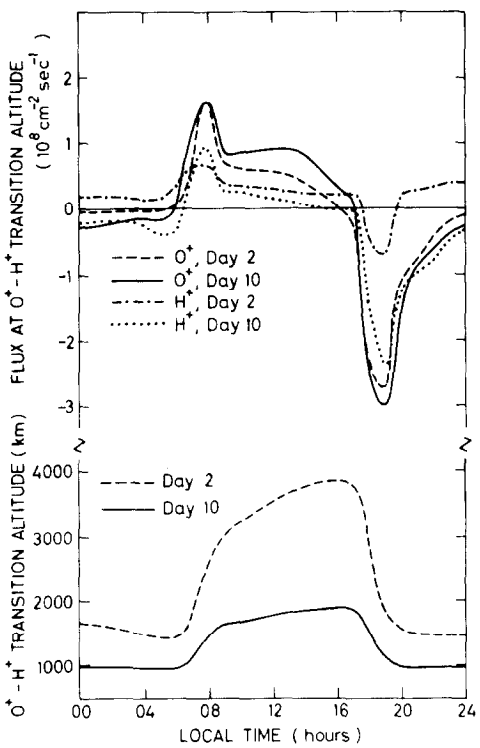

FIG. 12. Calculated daily behaviour of the O^+–H^+ transition altitude and the O^+ and H^+ fluxes at this altitude for Day 2 and Day 10.

the F2-region. Figure 8 shows the daily variation of NmF2 for Days 2 and 10. The Day 10 values of NmF2 are greater than the Day 2 values because the protonosphere is at a more advanced stage of replenishment. Also shown in Fig. 8 is the daily variation of hmF2, the altitude of NmF2. There is no day-to-day change in hmF2 after Day 2 of the calculations. This is to be expected since its value is controlled mainly by the O^+ diffusion coefficient, the O^+ loss rate coefficient and the meridional component of the neutral air wind. At F2-region altitudes there is no day-to-day change in these coefficients. Shown in Figs. 9 and 10 are contours with respect to time and altitude of the O^+ and H^+ concentrations, respectively, for Day 10 of the calculations.

Figure 11 shows the effect the day-to-day altitude changes in the O^+ and H^+ concentration have on the O^+–H^+ transition altitude. The day-to-day lowering of the O^+–H^+ transition altitude is due to the increase in the H^+ concentration at the higher altitudes as the protonosphere is replenished, whereas there is little day-to-day change in the O^+ concentrations. The effect of a more replenished protonosphere on the O^+ and H^+ field-aligned fluxes through the base of the protonosphere is shown in Fig. 12. We have taken, as mentioned in Section 1, the O^+–H^+ transition altitude to be the base of the protonosphere.

8. Conclusions

A method has been presented to solve the coupled time-dependent O^+ and H^+ continuity and momentum equations that apply in mid-latitude magnetic flux tubes extending from the lower boundary of the Earth's ionospheric F2-region to the equatorial plane. For the H^+ equations a "self-diffusion coefficient" is employed, which arises from a rearrangement of the H^+ momentum equation. An important advantage of using such a diffusion coefficient is the saving in computing time that can be achived with little difference in the solution. All the results presented apply to the $L = 3.2$ magnetic field line although test calculations have shown that the method is suitable for both lower and higher values of L. We have used data appropriate to equinox under sunspot maximum conditions. For illustration we have presented results from calculations obtained during the first few days of a post-magnetic storm recovery period of the protonosphere. In particular, we have shown that the H^+ content of the magnetic flux tube continually increases for several days during the early stages of post-magnetic storm recovery. It is most unlikely that the mid-latitude protonosphere will ever fully recover during the period between magnetic storms during sunspot maximum.

Acknowledgments

Thanks are due to J. V. Evans and J. E. Salah for supplying plasma temperature data, to R. J. Moffett and J. A. Murphy for helpful discussions and to Linda Wilkinson for writing a very useful graph plotting computer program.

REFERENCES

1. J. V. EVANS, *Rev. Geophys. Space Phys.* **13** (1975), 877.
2. J. A. MURPHY, G. J. BAILEY, AND R. J. MOFFETT, *J. Atmos. Terr. Phys.* **38** (1976), 351.
3. P. C. KENDALL AND W. M. PICKERING, *Planet. Space Sci.* **15** (1967), 825.
4. H. G. MAYR, E. G. FONTHEIM, L. H. BRACE, H. C. BRINTON, AND H. A. TAYLOR, JR., *J. Atmos. Terr. Phys.* **34** (1972), 1659.
5. R. J. MOFFETT AND J. A. MURPHY, *Planet. Space Sci.* **21** (1973), 43.
6. J. L. MASSA, Ph.D. thesis, University of Michigan, 1974.
7. G. J. BAILEY, *Planet. Space Sci.* **28** (1980), 47.
8. E. R. YOUNG, P. G. RICHARDS, AND D. G. TORR, to be published.
9. J. CRANK AND P. NICOLSON, *Proc. Cambridge Philos. Soc.* **43** (1947), 50.
10. P. LAASONEN, *Acta Math.* **31** (1949), 309.
11. G. J. BAILEY, R. J. MOFFETT, AND J. A. MURPHY, *Planet. Space Sci.* **26** (1978), 753.
12. C. G. PARK, *J. Geophys. Res.* **79** (1974), 169.
13. J. C. G. WALKER, *J. Atmos. Sci.* **22** (1965), 462.
14. L. G. JACCHIA, *Smithsonian Contr. Astrophy.* **8** (1965), 215.
15. L. G. JACCHIA, *Smithsonian Astrophys. Obs. Spec. Rep.* No. 332, 1971.
16. A. VIDAL-MADJAR, J. E. BLAMONT, AND B. PHISSAMAY, *J. Geophys. Res.* **79** (1974), 233.
17. K. MARUBASHI AND J. M. GREBOWSKY, *J. Geophys. Res.* **81** (1976), 1700.
18. G. P. SERBU AND E. J. R. MAIER, *J. Geophys. Res.* **75** (1970), 6102.
19. W. J. RAITT, R. W. SCHUNK, AND P. M. BANKS, *Planet. Space Sci.* **23** (1975), 1103.
20. R. G. ROBLE, *Planet. Space Sci.* **23** (1975), 1017.
21. R. W. SCHUNK AND J. C. G. WALKER, *Planet. Space Sci.* **17** (1969), 853.
22. R. G. ROBLE, B. A. EMERY, J. E. SALAH, AND P. B. HAYS, *J. Geophys. Res.* **79** (1974), 2868.
23. P. M. BANKS, A. F. NAGY, AND W. I. AXFORD, *Planet. Space Sci.* **19** (1971), 1053.
24. C. G. PARK, D. L. CARPENTER, AND D. B. WIGGIN, *J. Geophys. Res.* **83** (1978), 3137.